Structure-Dynamic Analysis of an Induction Machine depending on Stator-Housing Coupling

C. Schlensok, M. van der Giet, M. Herranz Gracia, D. van Riesen, K. Hameyer
Institute of Electrical Machines
RWTH Aachen University
Schinkelstr. 4, D-52062 Aachen, Germany
Email: dirk.vanriesen@iem.rwth-aachen.de

***Abstract*—The estimation and calculation of the acoustic sound of electric machinery is nowadays of particular interest. Various approaches have been presented relying either on analytical or on numerical models. In general, the analytical models are based on the electromagnetic-field theory and the results are compared to measurements. Numerical models allow for the separation of different exciting forces stemming from various effects. In the studied case of an induction motor with squirrel-cage rotor three effects are taken into account in the analytical model: the fundamental field, saturation, and eccentricity. The numerical analysis is applied to the analysis of acoustic sound of an electric machine. Nevertheless, the numerical results have to be verified. Hence, they are compared to the physically based analytical results. The radiated noise depends directly on the surface' deformation of the machine. Therefore, the analysis is focused on the structure-dynamic vibrations. The combined analysis presented here, allows for the reduction of vibrations and noise optimizing the coupling of the machine's stator and housing. Here, an Induction Machine (IM) with squirrel-cage rotor is studied. Its housing is mounted with six spiral-steel springs to the stator. With the presented method the impact of different numbers of springs is analyzed.**

I. Introduction

There have been several contribution to both, the analytical [1]–[3] and numerical [4]–[6] approach of estimating the radiated noise of electrical machinery. A comparison as well as a combination of both methods allows for more reliable predictions and faster improvements of the machine's structure. In this paper an Induction Machine (IM) with squirrel-cage rotor is studied by means of analytical and numerical methods. At first the applied models are introduced. In general, the structure of an IM is not purely cylindrical as the analytical models of [1]- [3] assume. For comparison reasons different numerical Finite-Element (FE) models are introduced and results are analyzed.

II. Analytical Model

The analytical model [1] is based on the analysis of the force-wave behavior resulting from the normal component of the air-gap flux-density B_n depending on space x and time t:

$$F_r(x,t) = \frac{B_n^2(x,t)}{2\mu_0} \tag{1}$$

with μ_0 being the magnetic field constant. $B_n^2(x,t)$ results from the fundamental and harmonic field of the stator interacting with the induced fundamental and harmonic field of the rotor. Three major effects are considered in the analytical model: The fundamental air-gap field, the saturation of the lamination and static and dynamic eccentricity. Each harmonic, i.e. each exciting force-wave frequency, results in oscillating space modes along the circumference of the stator at the air gap. The mode numbers r depend on the origin of the interacting field components of stator and rotor.

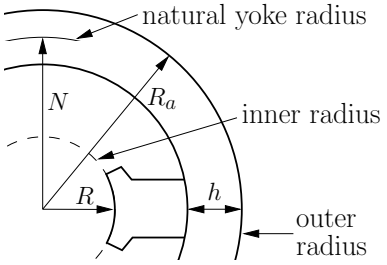

Fig. 1. Simplified analytical model of IM with teeth.

These force waves excite the structure of the machine, i.e. stator and housing. The analytical model simplifies the machine's structure to a cylindric ring as described in Fig. 1. In order to include the effect of slotting, the cylinder-ring model is modified taking the teeth into account introducing the adjusting factor

$$\Delta = \frac{\text{yoke weight}}{\text{tooth weight} + \text{yoke weight}}\,. \tag{2}$$

The weight of yoke and teeth is the equivalent to the corresponding cross sections. The eigenfrequency of $r = 0$ reads

$$F_0 = \frac{C_s}{2\pi \cdot N \cdot \sqrt{\Delta}} \tag{3}$$

with

$$C_s = \sqrt{\frac{E}{\rho}} \tag{4}$$

C_s is calculated taking the mass density ρ and Young's modulus E into account. With the analytical model the deformation magnitude of the analyzed oscillation mode r is estimated on the outer radius of the stator R_a. For this, the static and dynamic deformation factor needs to be calculated for an adequate cylinder ring. Since $r = 0$ results in pure tensile stress the static deformation is calculated to

$$Y_{0,stat} = \frac{R \cdot N}{E \cdot h} \cdot \sigma(f, r = 0)\,, \tag{5}$$

TABLE I
STATIC DEFORMATION FACTORS FOR DIFFERENT MODES r.

r	0	1	2	3	4	5	6
$\eta_{r,stat}$	1.0	596.4	35.7	5.0	1.4	0.6	0.3

with the natural yoke radius N, the height of the yoke h, and the inner radius of the stator R. The static deformation for mode number $r \geq 2$ are estimated with

$$Y_{r,stat} = \frac{R \cdot N}{E \cdot h} \cdot \frac{\sigma}{i^2(r^2-1)^2} \qquad \text{for} \quad r \geq 2 \tag{6}$$

with

$$i = \left(\frac{1}{2\sqrt{3}}\right) \cdot \left(\frac{h}{N}\right) . \tag{7}$$

The static factor as ratio of $\frac{Y_{r,stat}}{Y_{0,stat}}$ reads:

$$\eta_{r,stat} = \frac{12}{(r^2-1)^2} \cdot \left(\frac{N}{h}\right)^2 \qquad \text{for} \quad r \geq 2\,. \tag{8}$$

Bending forces are generated by $r = 1$. In this special case the corresponding static factor reads

$$\eta_{1,stat} = \frac{4}{3} \frac{h \cdot l_{Fe}}{N \cdot \left(\frac{d}{L}\right)^4 \cdot L}\,, \tag{9}$$

where l_{Fe} is the effective stack length and L the distance between both bearings. For $r \geq 1$ the factors given above are multiples of the deformation calculated for $r = 0$. Table I resumes the calculated static deformation factors for the studied IM.

The relative sensitivity of the structure γ is defined as the ratio of the force-wave harmonic f_r and the eigenfrequency F_0. With this and the bending and longitudinal oscillation frequencies f_r^B and f_r^L respectively, the dynamic factor reads:

$$\eta_{r,dyn} = \frac{r^2 - \gamma^2}{\left[\gamma^2 - \left(\frac{f_r^B}{F_0}\right)^2\right] \cdot \left[\gamma^2 - \left(\frac{f_r^L}{F_0}\right)^2\right]} \qquad \text{for} \quad r \geq 2\,. \tag{10}$$

In the special case $r = 1$, the lowest bending eigenfrequency is of interest:

$$F''_{b1} = \frac{1}{2\pi}\sqrt{\frac{c''_1}{m''}}\,. \tag{11}$$

For a machine with the shaft diameter d the spring constant c''_1 and the adequate mass m'' read:

$$c''_1 = \frac{3\pi}{4} \cdot E \cdot \left(\frac{d}{L}\right)^4 \cdot L. \tag{12}$$

The adequate mass m'' is calculated by

$$m'' = \rho_{Fe} \cdot \left\{ l\left[(2R)^2 - d^2\right] + \frac{1}{2} \cdot L \cdot d^2 \right\}, \tag{13}$$

with the mass density ρ_{Fe} of the rotor. The dynamic deformation factor $r = 1$ reads:

$$\eta_{1,dyn} = \frac{1}{1 - \gamma^2 \cdot \left(\frac{F_0}{F''_{b1}}\right)^2}\,. \tag{14}$$

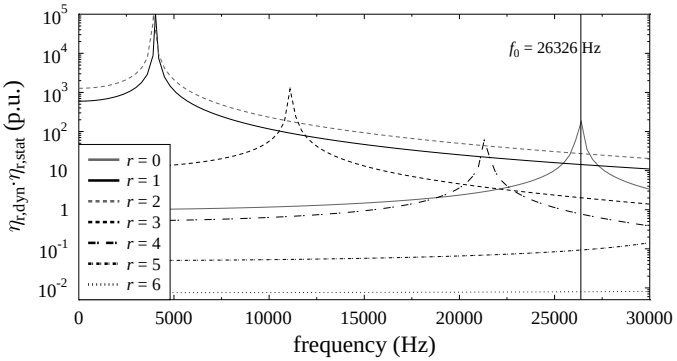

(a) Resulting factor $\eta_{stat} \cdot \eta_{dyn}(r)$.

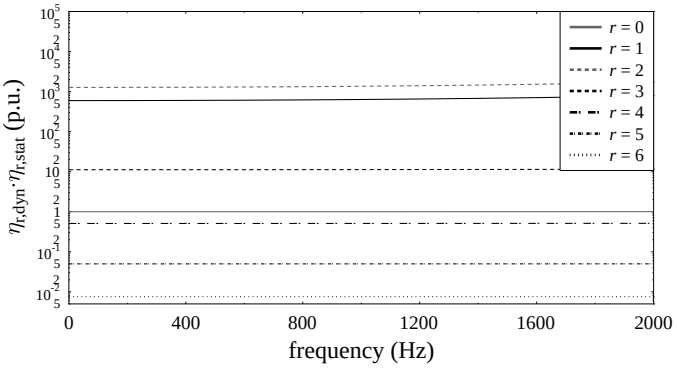

(b) Resulting factor $\eta_{stat} \cdot \eta_{dyn}(r)$ in analyzed frequency range.

Fig. 2. Resulting factor $\eta_{stat} \cdot \eta_{dyn}(r)$.

Finally, the overall deformation amplitude is calculated by

$$Y_r = \eta_{r,stat} \cdot \eta_{r,dynamic} \cdot Y_{0,stat}\,. \tag{15}$$

Fig. 2(a) shows the resulting behavior of the factor $\eta_{stat} \cdot \eta_{dyn}(r)$. Each mode number r shows a resonance. Due to the small size of the studied IM (800 W) these resonance frequencies are rather high. For $r \geq 4$ they are beyond the human ear's hearing ability. Next to this the modes $r \geq 3$ produce rather small amplification factors throughout the spectrum. For the analysis of the studied machine, the spectrum is reduced to $f_{max} = 1200$ Hz. Here, the entire range of frequencies shows constant amplifications for all modes as Fig. 2(b) shows. Therefore, the analysis of the deformation is reduced to small mode numbers $r \leq 10$. In case there are even two modes at the same frequency, the amplification factor decides, which of whom is important and which is negligible.

III. NUMERICAL MODEL

The Finite-Element model (FE) of the studied IM includes all mechanical parts of the machine as Fig. 3 shows. This complicated structure of the IM does not correspond exactly to the cylindrical analytical model. The simple model consists of the stator with winding. The numerical model provides the deformation for all nodes of the FE-model. After discretizing, the following oscillation equation is obtained:

$$\left(K + j\omega C - \omega^2 M\right) \cdot D = F\,. \tag{16}$$

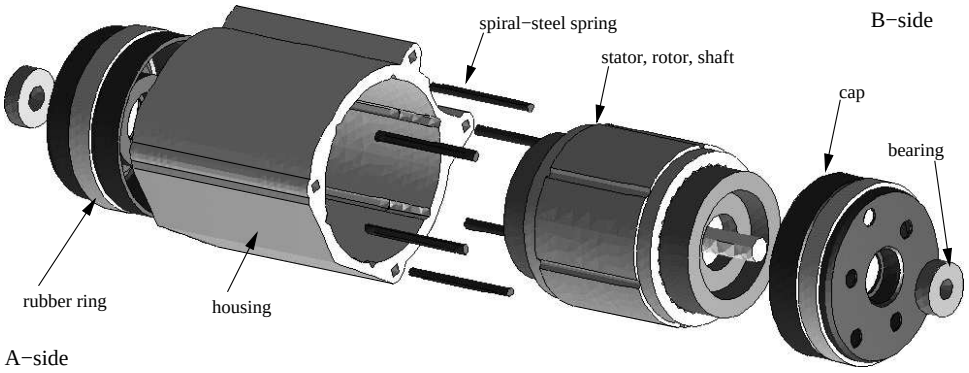

Fig. 3. Mechanical FE-model (exploded view).

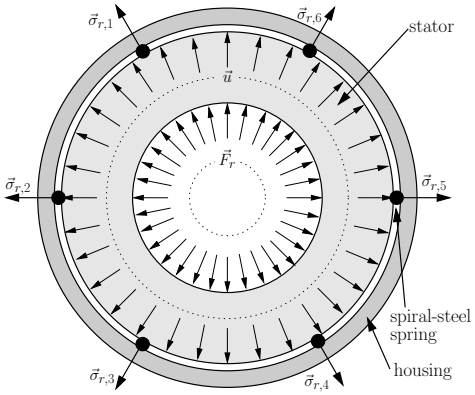

Fig. 4. Sampling of the stator deformation at location of springs.

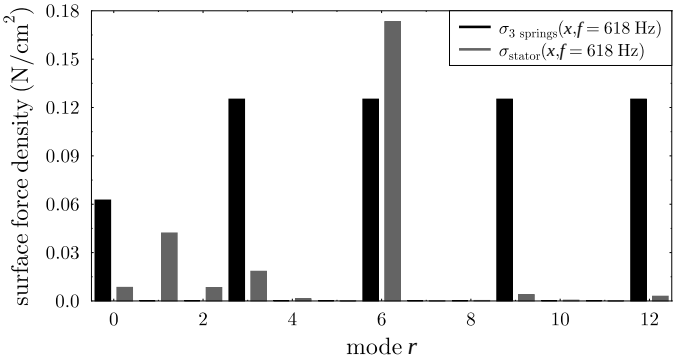

Fig. 5. Aliasing effect changing the exciting modes on the housing.

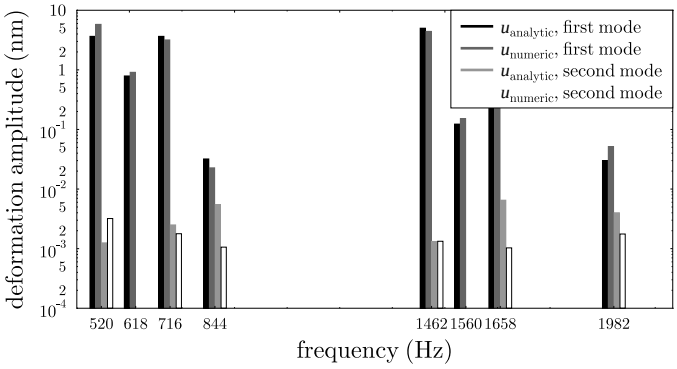

Fig. 6. Comparison of deformation amplitudes for models without housing.

In a second step of this study, the numerical model is modified applying the entire machine structure as shown in Fig. 3. In order to compare the results of both, the analytical and numerical model, the analytical is re-applied for the housing. For this, the deformation of the stator on the outer radius R_a is sampled, depending on the number of spiral-steel springs (Fig. 4). With the deformation samples the force excitation of the housing is calculated applying Hooke's law:

$$\sigma = E \cdot \epsilon \qquad \text{and} \qquad \epsilon = \frac{\Delta l}{l}\,. \tag{17}$$

$l = h$ is the height of the stator yoke and Δl the value of the deformation at the location of the spiral-steel spring. The sampling can either be performed with the FE-model or the analytical model. After sampling, σ is transformed to the space domain providing the appearing modes of force excitation $r(\sigma)$. Due to the sampling, aliasing appears, depending on the original mode number. Fig. 5 shows the sampling and resulting mode numbers for $f = 618\,\text{Hz}$ exemplarily. The stator deformation shows a strong mode $r = 6$. In the case of three spiral-steel springs, the most significant mode numbers are $r = 0$ and 3, respectively.

IV. Results

At first, the results of the analytical and numerical models without housing are compared. The deformation is analyzed by separating the modes r. By this, the impact of the mode number can be studied as well. Resuming the deformation values for some selected frequencies, Fig. 6 shows, that in the case of two significant modes of the exciting surface-force density the lower mode number has a significantly higher impact in any case. At $f = 844\,\text{Hz}$ for example, the mode numbers $r = 4$ and 8 occur, the latter having the higher force magnitude. Nevertheless, $r = 4$ reaches the higher deformation amplitude by a factor of 5.8. It can be stated that in general, if two modes appear the higher can be neglected [1]. The only exception is the case of $r = 0$, which might produce lower deformation than $r = 1$ and 2. Next to this, Fig. 6 shows very good agreement of the analytical and numerical models. Since the analytical model has been verified

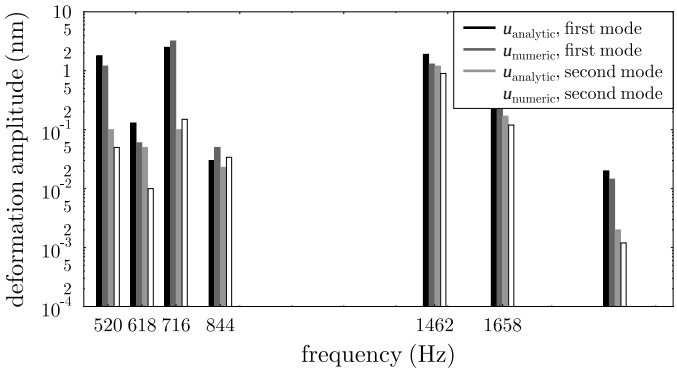

Fig. 7. Comparison of deformation amplitudes for models with housing.

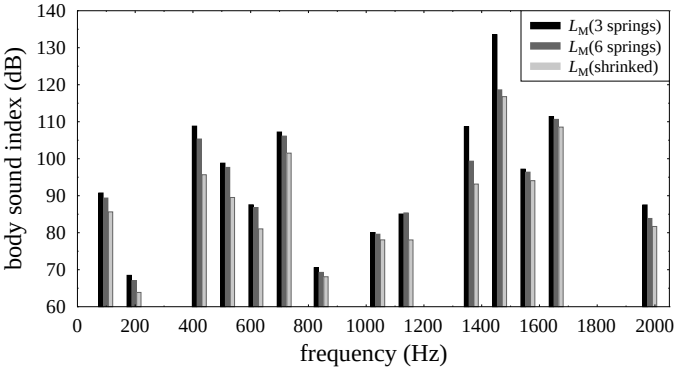

Fig. 8. Comparison of different stator-to-housing couplings.

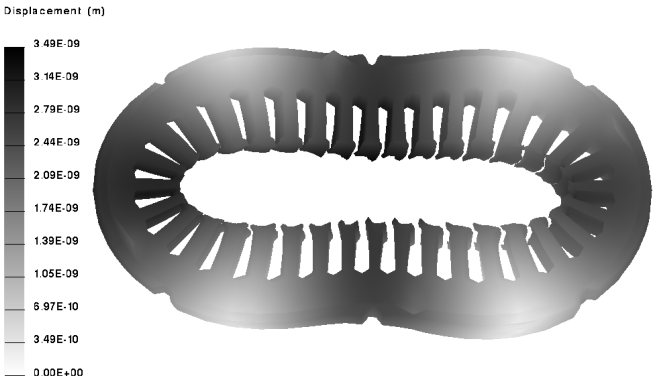

Fig. 9. Deformation of stator at 1462 Hz for 6-pin model.

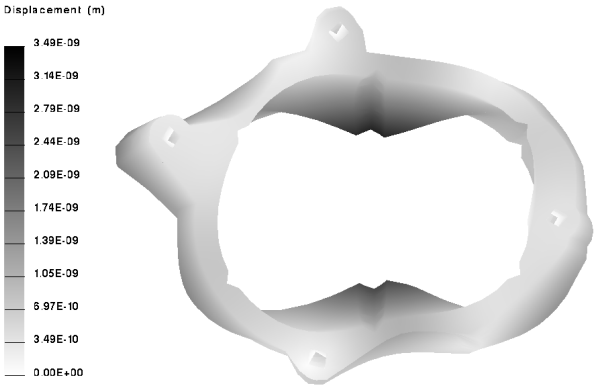

Fig. 10. Deformation of housing at 1462 Hz for 6-pin model.

by measurements many times before [1] the numerical model is stated to be reliable.

Finally, the mechanical deformation is simulated for the machine model with the entire detailed structure (Fig. 3). In this way, the impact of different stator-to-housing couplings is analyzed. Three models are studied: A model with 3 another with 6 spiral-steel springs and one with a shrinked stator, equivalent to an infinite number of springs is studied. Fig. 7 compares the analytical and numerical models with 6 springs.

Two effects can be stated: The first is, that the housing increasing the stiffness of the machine as an additional mass, i.e. the height of the cylinder ring increases (Fig. 1), and it reduces the maximum deformation. On the other hand, the aliasing effect shown in Fig. 5 results in smaller and additional mode numbers producing larger deformation. Both effects are detected in Fig. 7. For example $f = 844\,\text{Hz}$ shows larger deformation values for the model with housing and six springs. This is due to the fact that the original mode number $r = 8$ is transmitted to $r = 1$ and 2. For $f = 520\,\text{Hz}$ the maximum deformation at mode $r = 2$ is reduced by more than $50\,\%$.

Fig. 8 shows the comparison of the three different stator-to-housing couplings applying the body-sound index L_M. It can be stated that for all analyzed frequencies the shrinked model results in the lowest deformation and vibration. Therefore, this variant will produce the lowest noise radiation. The variant with 3 springs is the worst and must be avoided.

Large deformation differences can be stated for 1462 Hz (cf. Fig. 8) regarding the models with 3 pins or 6 pins coupling the stator to the housing. For this frequency, deformation and mode results are presented in more detail in the following section.

Figs. 9 and 10 show the deformation of stator and housing for the frequency 1462 Hz for the model with 6 pins. A very strong mode 2 deformation can be stated. The same evaluation is performed for the model with 3 pins. The results are depicted in Fig. 11 and 12 for the stator and the housing respectively. Here, the same force excitation leads to a dominant mode with $r = 1$. Additionally, it can be read from the scale that the maximum deformation amplitude is higher, as if was expected from the results in Fig. 8.

Figs. 13 and 14 summarize the deformation modes for the model with 6 pins and the model with 3 pins. Here, the dominant mode $r = 2$ can be seen for the model with 6 pins. The model with 3 pins does not show this mode due to aliasing effects, here the deformation stemming from the force excitation in the stator is translated almost entirely to a mode $r = 1$.

V. Optimization of the Coupling Between Stator and Housing

In the previous section, it has been demonstrated that shrinking results in the lowest deformation amplitudes. Due

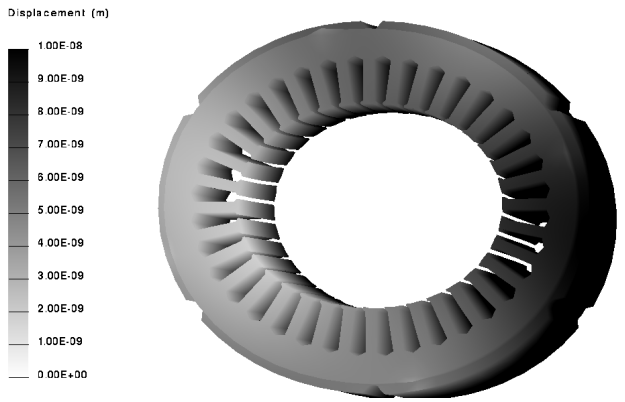

Fig. 11. Deformation of stator at 1462 Hz for 3-pin model.

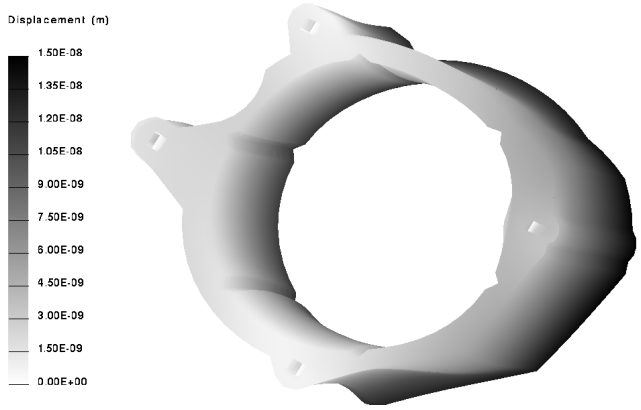

Fig. 12. Deformation of housing at 1462 Hz for 3-pin model.

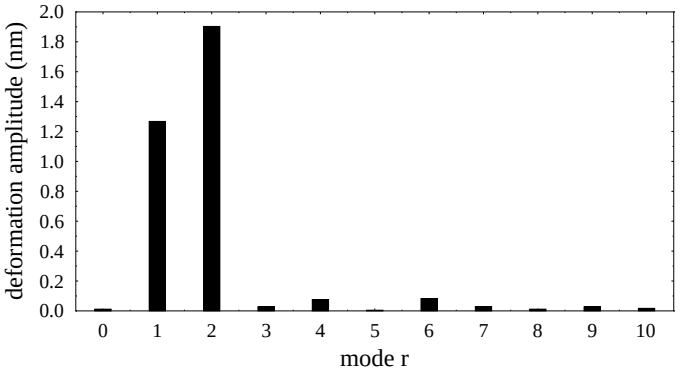

Fig. 13. Modes at 1462 Hz for 6-pin model.

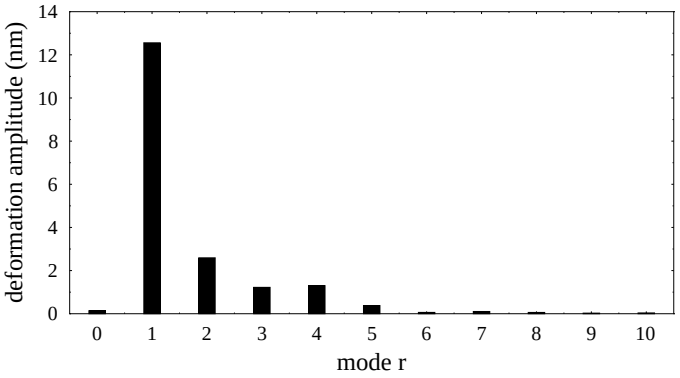

Fig. 14. Modes at 1462 Hz for 3-pin model.

to manufacturing reasons the coupling through spiral-steel springs is normally preferred. Therefore, a procedure, which determines the optimum number and distribution of the spiral-steel springs is needed.

This optimization is performed under the following assumptions:

- The housing is cylindrical and the spiral-steel springs are distributed in the inner radius of the housing.
- The spiral-steel springs transmit the force excitation from stator to housing at one point, ideally.
- The mechanical behavior of the housing has no influence on the mechanical behavior of the stator.

The objective of this optimization is the minimization of the sound intensity level L_f for the frequency that generates its maximum value:

$$Z = min[max[L_{I_f}]]. \tag{18}$$

The value of the sound intensity level for each frequency is defined as

$$L_{I_f} = 10 \cdot \log \frac{I_f}{I_{sf}}, \tag{19}$$

where I_{sf} is the threshold value for the human ear of the sound intensity for the frequency f. I_f is the sound intensity generated by the deformation on the surface of the housing with frequency f. For points at a distance d from the surface of the housing, I_f can be calculated as

$$I_f = k \cdot \frac{u_f^2 \cdot f^4}{d^2}, \tag{20}$$

where k is a constant, which dependents on the radiation characteristics of the machine and u_f the amplitude of the displacement with frequency f. The displacement of the housing is equal to the sum for all significant mode numbers of the deformation amplitude, which is calculated using the analytical model as follows

$$u_f = \sum_{r=0}^{r_{max}} Y_r = \sum_{r=0}^{r_{max}} \frac{R \cdot N}{E \cdot h} \eta_{r,stat} \cdot \eta_{r,dyn,f} \cdot \sigma_{r,f}, \tag{21}$$

where $\sigma_{r,f}$ is the force excitation for mode number r and frequency f transmitted from stator to the inner radius of the housing through the spiral-steel springs.

The force excitation through the inner radius of the housing for f is

$$\sigma_f(x) = \sum_{i=1}^{N_{sp}} \sigma_{i,f} \cdot \delta(x - x_i), \tag{22}$$

where N_{sp} is the number of spiral-steel springs and $\sigma_{i,f}$ the force excitation in stator in the position of the spring and, which is transmitted completely to the housing. $\delta(x)$ is the unit impulse function and x_i is the position along

the circumference of each spring, which in the case of a symmetrically distribution can be written as

$$x_i = \alpha + i\frac{2\pi}{N_{sp}}, \tag{23}$$

where α is the position of the first spring. $\sigma_f(x)$ can be expressed as a Fourier series with the following coefficients

$$a_{r,f} = \frac{1}{\pi}\sum_{i=1}^{N_{sp}} \sigma_{i,f} \cdot \cos(r \cdot x_i) \tag{24}$$

$$b_{r,f} = \frac{1}{\pi}\sum_{i=1}^{N_{sp}} \sigma_{i,f} \cdot \sin(r \cdot x_i) \tag{25}$$

$$\sigma_{r,f} = \sqrt{a_{r,f}^2 + b_{r,f}^2} \tag{26}$$

The latter can be used as input data for the calculation of the displacement of the housing, see (21).

Once the objective function for the optimization is defined, three different approaches according to the optimization parameters are possible:

- The spiral-steel springs are distributed symmetrically at the stator outer radius and the influence of the position of the first spring is neglected ($\alpha = 0$). In this case, the only optimization parameter is the number of springs N_{sp} and the only constraints are that the number of springs should be a natural number and that due to practical reasons it has to be between 2 and 20.

$$N_{sp} \in \mathbb{N} \text{ and} \tag{27}$$

$$2 \leq N_{sp} \leq 20. \tag{28}$$

  In this case, the one-dimensional optimization can be easily solved by trying all possibilities.
- The spiral-steel springs are distributed symmetrically at the stator outer radius and the influence of the position of the first spring α is taken into account. This results in a mixed optimization with two optimization parameters:
  - the number of spiral-steel springs, with the same constraints as in the previous case and
  - the position of the first spring α, with the constraints

$$\alpha \in \mathbb{R} \text{ and} \tag{29}$$

$$0 \leq \alpha < \frac{2\pi}{N_{sp}}. \tag{30}$$

  This mixed two-dimensional optimization can be solved using an optimization algorithms such as differential evolution [8].
- The spiral-steel springs are allowed to be distributed unsymmetrically. This results in two types of optimization parameters:
  - the number of spiral-steel springs, with the known constraints and
  - the position of each of the strings

$$x_i,\ i = 1 \ldots N_{sp}. \tag{31}$$

    The constraints applying to each of these variables are:

$$x_i \in \mathbb{R}^+ \text{ and} \tag{32}$$

$$x_i \neq x_j,\ j = 1 \ldots i. \tag{33}$$

    The second constraint forbids that two springs have the same position.

  In this case, the number of optimization parameters depends on the value of one of these parameters (N_{sp}). Therefore, it is not possible to apply directly an optimization algorithms. Taking advantage of the fact that N_{sp} can only take 18 different values, the optimization of the positions of the springs can be done for each value of N_{sp} and the global optimum will be the best of the local optima.

The third case is the most general one and the solution of it is sure to be the global optimum, because the possible optima for the first two cases are only a restriction of the possible optima for the third case. This means that it is possible that the optimization of the spring distribution results in a symmetrical distribution such as is assumed in the first and second cases. The optimization effort in the third case is of course also higher.

VI. Conclusion

The presented paper reviews the analytical theory of [1] and verifies the introduced numerical structure-dynamic model. The analysis of the deformational modes shows, that small mode numbers have the strongest impact by far. The coupling of housing and stator should either apply shrinking or and adequate number of spiral-steel springs. Moreover, a generalized procedure to optimize this coupling is presented and the necessary optimization effort is discussed for different assumptions about the coupling. Further results of this optimization will be presented in future works.

References

[1] H. Jordan, *Geräuscharme Elektromotoren*. Essen: Verlag W. Girardet, 1950.

[2] P. L. Timar, *Noise and Vibration on Electrical Machines*. New York: Elsevier Science Publishing Company, 1998.

[3] S. L. Nau, "Acoustic noise of induction electric motor: Causes and solutions," in *2nd International Seminar on Vibrations and Acoustic Noise of Electric Machinery*. Łódź, Poland: VANEM, September 2000, pp. 173–178.

[4] O. C. Zienkiewicz and R. L. Taylor, *The finite element method*. London: McGraw-Hill Book Company, 1989.

[5] J. F. Gieras, C. Wang and J. C. Lai, Noise of Polyphase Electric Motors, CRC, 2005.

[6] L. Vandevelde, J. J. C. Gyselinck, F. Bokose, and J. A. A. Melkebeek, "Vibrations of magnetic origin of switched reluctance motors," *COMPEL*, vol. 22, no. 4, pp. 1009–1020, Nov 2003.

[7] C. Schlensok, D. van Riesen, T. Küest, and G. Henneberger, "Acoustic simulation of an induction machine with squirrel-cage rotor," *COMPEL*, vol. 25, no. 2, pp. 475–486, March 2006.

[8] K. Hameyer, *Numerical Modelling and Design of Electrical Machines and Devices*. Southampton, Boston: WITPress, 1999.